Pellet and Pellet-Blanket Time-Dependent and Time-Integrated Neutronics and Photonics for Electron-Beam-Fusion Microexplosions

M.M.H. Ragheb, G. Moses, and C.W. Maynard

May 1979

UWFDM-295

FUSION TECHNOLOGY INSTITUTE

UNIVERSITY OF WISCONSIN

MADISON WISCONSIN

Pellet and Pellet-Blanket Time-Dependent and Time-Integrated Neutronics and Photonics for Electron-Beam-Fusion Microexplosions

M.M.H. Ragheb, G. Moses, and C.W. Maynard

Fusion Technology Institute
University of Wisconsin
1500 Engineering Drive
Madison, WI 53706

http://fti.neep.wisc.edu

May 1979

UWFDM-295

PELLET AND PELLET-BLANKET NEUTRONICS AND PHOTONICS FOR ELECTRON-BEAM-FUSION MICROEXPLOSIONS

Magdi M.H. Ragheb
Gregory A. Moses
Charles W. Maynard

Fusion Engineering Program
Nuclear Engineering Department
University of Wisconsin
Madison WI 53706

July 1979

UWFDM-295

Contents

Abstract

Pellet and coupled pellet-blanket time-integrated neutronics and photonics calculations are reported for a representative low gain (25), low compression (ρr = 0.94) pellet design for an electron beam fusion reactor. Tungsten, lead and natural U are compared as pusher-tamper materials. In the three cases, neutron balances show that neutron multiplication in the pellet compensates for the energy losses and spectral softening due to neutron interactions. Fissile breeding cannot be achieved in the natural U case, since the fission reaction predominates. Substantive additional energy can be obtained (~5.5 MeV/source neutron) in the pellet if natural U is used as the tamper material. Neutron and gamma spectra from the pellet microexplosions are given. Natural U, W and Pb cause 14%, 7% and 4% neutron multiplication, respectively. Compared to the case where a pure 14.1 MeV source is used, the spectra for the Pb and W pellets lead to almost the same values of breeding and heating rates. However, these are apportioned differently between the $Li^6(n,\alpha)$ and $^7Li(n,n'\alpha)$ reactions and spatial positions in the blanket. The atomic displacements and the gas production per unit of thermal power produced, at the first wall are substantially reduced in the natural U case. Natural U as a tamper material leads to 8% higher tritium breeding, and a 39% increase in energy production compared to the W case. Per unit of energy produced, it leads to 27% less displacement damage, and 30% less H and He production than the W pellet case. For larger ρr values, these effects may be more pronounced. These results indicate that longer wall lifetimes may be obtained by neutron spectrum softening in the pellet without affecting the breeding and heat production in the blanket.

I. Introduction

Because of their efficiency (25-30%), simplicity, smaller size and low cost (~2% of lasers of comparable energy), high-energy, electron-beam accelerators are now being considered for inertial confinement fusion.[1,2] Electron beams can be bent by either magnetic fields or by bending the initial ionization path, keeping the diodes out of the line of sight of the 14.1 MeV neutrons produced. The radiation streaming and damage to the last mirror problems encountered in laser reactor designs can thus be avoided.[3]

In the inertial approach to nuclear fusion, deuterium-tritium (D-T) fuel is heated as it is compressed by laser, electron, or ion beams to extreme densities (~ 100-1000 times the fuel solid density). The compressed fuel being restrained by its own inertia, burns; before flying apart in a microexplosion, in less than a billionth of a second.[1] The compression is caused by a rocketlike ablation of the pellet surface and an implosion of the D-T fuel at the center of the pellet. The compression both heats the fuel to the ignition temperature and increases the amount of fuel that can be burned. The heating is caused by the $\int PdV$ compressive work of the implosion, generating kinetic energy which is converted nearly isentropically to internal energy in the compressed volume. The burn rate in the pellet is proportional to the density, ρ, and $\overline{\sigma v}$, the Maxwellian velocity-averaged reaction cross-section The confinement time is proportional to the radius divided by the sound speed.[4] Thus, the burn efficiency is proportional to the product of density and radius, ρr. In spherical compression, an x-fold reduction in the radius causes an x^3-fold increase in the density, which results in an x^2-fold increase in the ρr product and the burn efficiency. The nuclide density is proportional to the mass density, thus reaction macroscopic cross sections are increased x^3 times, and mean free paths are consequently decreased by an x^3 factor. Hence, the optical thicknesses for particle tracks (neutrons, gammas) may be comparable

to the actual pellet physical dimensions.

Particle beam pellets are expect to be larger and more massive (perhaps a half cm in radius) than laser targets because of the greater range of high-energy electrons and light ions in materials compared to photons, the focussing limitations of energetic charged particles and the longer duration of the pulses. The outer part of the pellet is composed of the ablator, a thin shell of high-Z material that is required to absorb the electron-beam energy. A velocity multiplier structured pellet would comprise a pusher that is imploded by the high pressure from the ablator. The pusher imparts its momentum to an inner tamper through a foam cushion. The tamper compresses and heats a D-T mixture at the center of the pellet. The input energy is accumulated over the implosion time and concentrated in the fuel only at the last stage of fuel collapse. The DT fuel is surrounded by a thermally insulating material such as tungsten or gold. The fuel implodes first, becomes a superheated spot at the center, and centrally ignites the rest of the fuel.

In this paper, the neutronics and photonics aspects of a representative electron beam pellet will be studied in Sec. II. Different pusher-tamper materials are considered and the corresponding particle spectra and neutron balances are compared. In Sec. III, coupled pellet-blanket neutronics and photonics are considered. Neutron and gamma heating rates, breeding rates and radiation damage phenomena are investigated. Conclusions and recommendations for future work are given.

II. Pellet Neutronics and Photonics

II.1. Introduction

Major differences exist between the neutronics and photonics treatment of magnetic and inertial confinement systems. In magnetic confinement, the

ion density in the plasma is so low ($\sim 10^{14}/cm^3$) that neutrons born in the plasma will reach the first wall practically without collisions at their initial 14.1 MeV energy. In inertial confinement, the ion number density is so high ($\sim 10^{26}/cm^3$) that one can expect the 14.1 MeV neutrons to sustain some elastic collisions in the D-T core. Inelastic collisions can also be expected with the high-Z materials used for the pusher-tamper-ablator system. This not only leads to a softening of the spectrum, but to the generation through inelastic reactions of γ-rays. The possibility of compensating for the absorption of neutrons in high-Z pellet components, by neutron-multiplying processes such as (n,2n), (n,3n) and fission reactions, and the breeding of fissile fuel in the pellet is investigated in this study. The softening of the spectrum will have an effect on the gas production rates in the blanket, breeding reactions, heating rate, and radiation damage rates. This is also studied for the case of a Li_2O blanket with a stainless steel structure.

The density profile, composition and configuration are continuously changing throughout the pellet burn, the source distribution is nonuniform (follows burn front), and the peak of the spatial distribution of the source is continually moving toward the outside of the pellet.[9] Accurate calculations would consider elaborate, coupled neutronics-photonics and hydrodynamic calculations.[6-10] However, since the burn time of the pellet (~10 ps) is much longer than the slowing down time of high-energy neutrons (~0.057 psec for 10 MeV neutrons at ρr = 1.2 g/cm^2), a constant source associated with a constant density profile of the pellet at the instant of burn starting can still yield very useful information.[9] The adopted model, results and methods used in our pellet calculations are discussed in the next sections.

II.2. Pellet Computational Model

For this study, a velocity-multiplier structured pellet with an iron ablator with the dimensions of Fig. 1 was considered as typical of a pellet

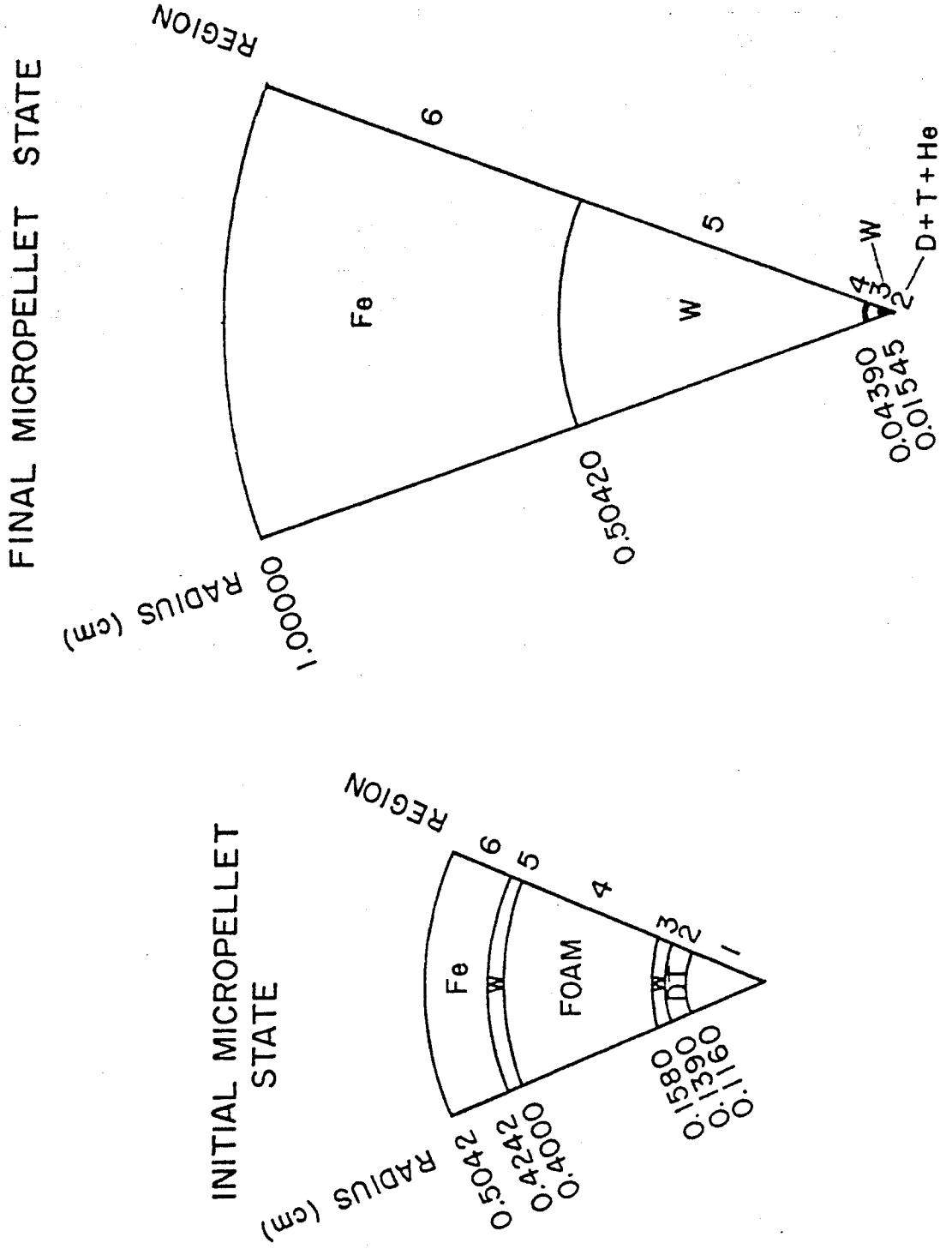
FINAL MICROPELLET STATE
REGION
RADIUS (cm)
Fe
W
D+T+He
6
5
4
3
2
1.00000
0.50420
0.04690
0.01545
INITIAL MICROPELLET STATE
REGION
RADIUS (cm)
Fe
W
FOAM
W
D
6
5
4
3
2
1
0.5042
0.4242
0.4000
0.1580
0.1390
0.1160

FIGURE 1

design for electron beam fusion reactor applications. Tungsten is shown in the figure as the pusher-tamper material. Pb and natural uranium were considered in our study as alternative materials, Pb for its neutron multiplication property by (n,2n) reactions, and natural U for the possible neutron multiplication by both (n,2n), (n,3n) and fast fission reactions, and the possibility of fissile breeding in the pellet itself rather than in the surrounding blanket. Gold, depleted Uranium, Tantalum or Rhenium can also be used instead of W.

Table 1 lists the density data for the estimated initial and final states of this pellet design. For an input energy of 4 MJ, the pellet gain is assumed to be 25, yielding an energy of 100 MJ per microexplosion. At a repetition rate of 1 Hz, and a fusion reaction yield of 17.6 MeV, such a 100 MW fusion power system would yield a 14.1 MeV source of strength:

$$S_n = 100\ \text{MW} \times 10^6 \frac{\text{W}}{\text{MW}} \times \frac{1}{1.6021 \times 10^{-13}} \frac{\text{MeV}}{\text{Joule}} \times \frac{1}{17.6\ \text{MeV}}$$

$$= 3.55 \times 19^{19}(14.1\ \text{MeV})\ \text{neutrons/sec.}$$

The cushion region and the cavity gas were not included in our modeling because few interactions were expected in them. For example, the total microscopic cross-section of Xe at 5 MeV is $\sigma_t \approx 5b$. At a pressure of 0.132 atm and a temperature of 20°C, the relationship, P = NkT, yields an atomic density of 3.29×10^{18} nuclei/cm^3. A mean free path can be calculated as $\lambda = 1/N\sigma_t = 608m$, which is quite large compared to the cavity radius of 5 m.

A version of the MORSE Monte Carlo code[11] with modifications to treat source driven multiplying media[12] was used for these calculations. A 25 neutron-21 gamma group cross-section set was used.[13] These were group collapsed from the Vitamin-C data library.[14]

Table 1 Pellet Data for the Initial and Final States

Initial State

Region	Composition	Volume(cm^3)	Initial Density (g/cm^3)	ρr (g/cm^2)	Material Weight(g)	Atomic Densities Atoms/(b·cm)
1	Void	6.54×10^{-3}	-	-	-	-
2	Frozen DT (50-50 atomic mixture	4.71×10^{-3}	0.213	4.90×10^{-3}	1.00×10^{-3}	$N_D = N_T = 2.55 \times 10^{-2}$
3	W Tamper	5.27×10^{-3}	19.300	3.67×10^{-1}	1.02×10^{-1}	$N_W = 6.32 \times 10^{-2}$
4	Foam Cushion	2.52×10^{-1}	-	-	-	-
5	W Pusher	5.17×10^{-2}	19.300	4.67×10^{-1}	9.98×10^{-1}	$N_W = 6.32 \times 10^{-2}$
6	Fe Ablator	2.17×10^{-1}	7.874	6.30×10^{-1}	1.71×10^{0}	$N_{Fe} = 8.49 \times 10^{-2}$
Sum		5.37×10^{-1}			2.81×10^{0}	

Imploded Final State

Region	Composition	Volume(cm^3)	Final Density (g/cm^3)	ρr (g/cm^2)	Material Weight(g)	Atomic Densities Atoms/(b·cm)
2	D + T + ^4He	1.54×10^{-5}	6.10×10^{1}	9.42×10^{-1}	2.80×10^{-4} 4.20×10^{-4} 2.40×10^{-4}	5.44×10^{0} 5.45×10^{0} 2.35×10^{0}
3	W	3.39×10^{-4}	3.01×10^{2}	8.56×10^{0}	1.02×10^{-1}	9.86×10^{-1}
5	W	5.37×10^{-1}	1.86×10^{0}	8.56×10^{-1}	9.98×10^{-1}	6.09×10^{-3}
6	Fe	3.65×10^{0}	4.68×10^{-1}	2.32×10^{-1}	1.71×10^{0}	5.05×10^{-3}
Sum		4.19×10^{0}			2.81×10^{0}	

The neutron source was sampled uniformly in the compressed pellet volume according to the probability density function:

$$p(r)dr = \frac{4\pi r^2 dr}{\int_0^R 4\pi r^2 dr},$$

where R is the compressed pellet radius. For a uniformly distributed random number ρ, a radius is sampled as:

$$r = R \cdot \rho^{1/3}.$$

Direction cosines were sampled isotropically.

Assuming the initial and final configurations would be the same as for the W pellet, pellets with Pb and natural U as pusher-tamper materials were investigated. Table 2 shows the data for different pellets for pusher-tamper region and Table 3 shows the corresponding atomic densities adopted in the calculations. Notice that the atomic densities are higher in the W case than in the natural U and Pb cases. On this basis, fewer interactions with the tamper can be expected in the Pb case than in the natural U and W cases.

Results of calculations follow in the next subsection.

II.3. Calculational Results

Neutron spectra from different pusher-tamper materials are displayed in Figs. 2-4. These all correspond to a DT core, $\rho r = 0.94$ g/cm^2, pellet. Different ρr values will lead to different spectra. The spectra are displayed in the four pellet regions: core, tamper, pusher and ablator. The spectrum in the ablator would be the spectrum falling on the first wall. It can be used as a source for further blanket calculations. It is incorrect to use it for first-wall calculations without first accounting for first wall and blanket interactions. The neutron spectra are tabulated in Table 4 for the reader wishing to use the ablator spectrum as a source for blanket calculations.

Table 2 Tamper-Pusher Data for Different Materials Choices. Initial and Final Pellet Dimensions Assumed the Same for Different Materials

Quantity	Region	W	Pb	Nat. U
Initial Volume (cm^3)	3	5.27×10^{-3}	5.27×10^{-3}	5.27×10^{-3}
(cm^3)	4	5.17×10^{-2}	5.17×10^{-2}	5.17×10^{-2}
Final Volume	3	3.39×10^{-4}	3.39×10^{-4}	3.39×10^{-4}
(cm^3)	4	5.37×10^{-1}	5.37×10^{-1}	5.37×10^{-1}
Initial Density (g/cm^3)		19.30×10^{0}	11.35×10^{0}	18.95×10^{0}
Initial Weight	3	1.02×10^{-1}	5.98×10^{-2}	9.99×10^{-2}
(g)	4	9.98×10^{-1}	5.87×10^{-1}	9.80×10^{-1}
Initial ρr	3	3.67×10^{-1}	2.16×10^{-1}	3.60×10^{-1}
(g/cm^2)	4	4.67×10^{-1}	2.75×10^{-1}	4.59×10^{-1}
Final Density	3	3.01×10^{2}	1.76×10^{2}	2.95×10^{2}
(g/cm^3)	4	1.86×10^{0}	1.09×10^{0}	1.82×10^{0}
Final ρr	3	8.56×10^{0}	5.01×10^{0}	8.39×10^{0}
(g/cm^2)	4	8.56×10^{-1}	5.02×10^{-1}	8.38×10^{-1}

Table 3 Atomic Densities for Different Pusher-Tamper Materials Considered, for Same Initial and Final Configurations

Region	Atomic Densities, Atoms/(b•cm)		
	W	Pb	Nat. U
3	$N(W)=9.860\times10^{-1}$ $N(^{182}W)=2.618\times10^{-1}$ $N(^{183}W)=1.420\times10^{-1}$ $N(^{184}W)=3.021\times10^{-1}$ $N(^{186}W)=2.801\times10^{-1}$	$N(Pb)=5.116\times10^{-1}$	$N(U)=7.464\times10^{-1}$ $N(^{238}U)=7.410\times10^{-1}$ $N(^{235}U)=5.374\times10^{-3}$
5	$N(W)=6.090\times10^{-3}$ $N(^{182}W)=1.617\times10^{-3}$ $N(^{183}W)=8.770\times10^{-4}$ $N(^{184}W)=1.866\times10^{-3}$ $N(^{186}W)=1.730\times10^{-3}$	$N(Pb)=3.168\times10^{-3}$	$N(U)=4.605\times10^{-3}$ $N(^{238}U)=4.572\times10^{-3}$ $N^{(235}U)=3.316\times10^{-5}$

Nat. U isotopic abundance: $^{234}U(0.0054\%)$, $^{235}U(0.72\%)$, $^{238}U(99.274\%)$

For our purposes: $^{235}U(0.72\%)$, $^{238}U(99.28\%)$

W isotopic abundance: $^{180}W(0.14\%)$, $^{182}W(26.41\%)$, $^{183}W(14.40\%)$, $^{184}W(30.64\%)$, $^{186}W(28.41\%)$

For our purposes: $^{182}W(26.55\%)$, $^{183}W(14.40\%)$, $^{184}W(30.64\%)$, $^{186}W(28.41\%)$

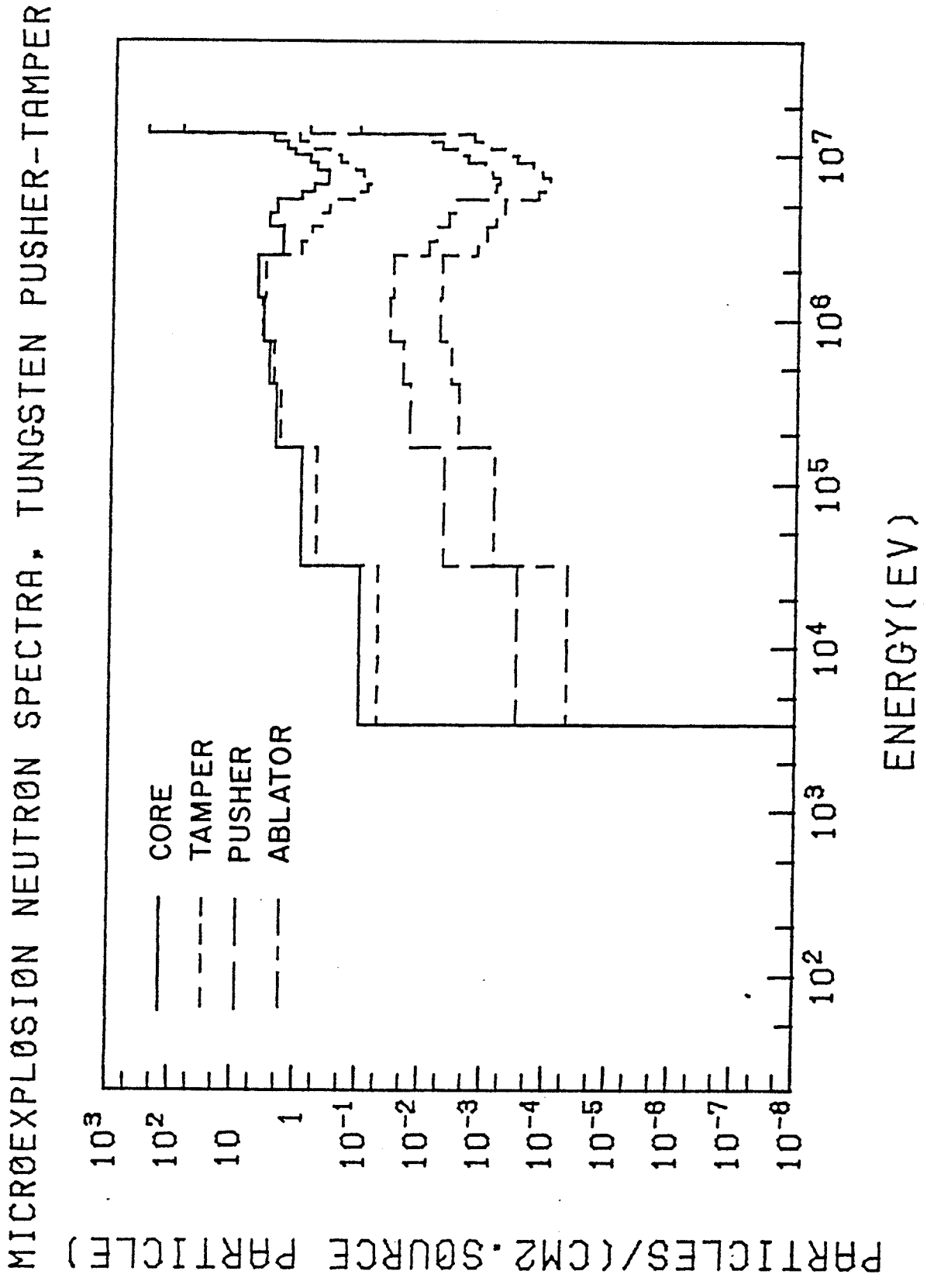
MICRØEXPLØSIØN NEUTRØN SPECTRA, TUNGSTEN PUSHER-TAMPER
PARTICLES/(CM2·SØURCE PARTICLE)
ENERGY(EV)
CORE
TAMPER
PUSHER
ABLATOR
10³
10²
10
1
10⁻¹
10⁻²
10⁻³
10⁻⁴
10⁻⁵
10⁻⁶
10⁻⁷
10⁻⁸
10²
10³
10⁴
10⁵
10⁶
10⁷

FIGURE 2

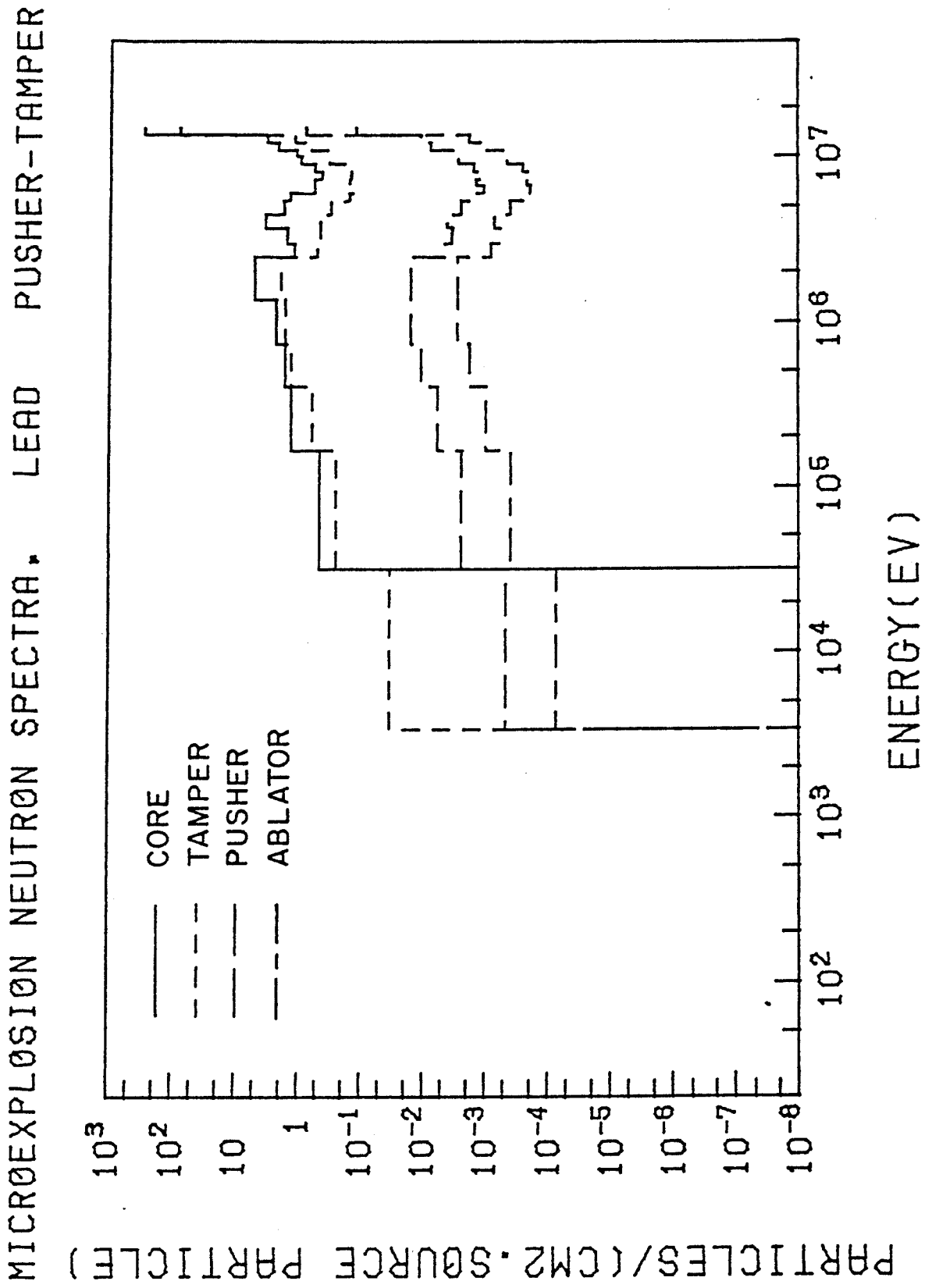
MICRØEXPLØSIØN NEUTRØN SPECTRA. LEAD PUSHER-TAMPER
CORE
TAMPER
PUSHER
ABLATOR
PARTICLES/(CM2·SOURCE PARTICLE)
ENERGY(EV)
10^3
10^2
10
1
10^-1
10^-2
10^-3
10^-4
10^-5
10^-6
10^-7
10^-8
10^2
10^3
10^4
10^5
10^6
10^7

FIGURE 3

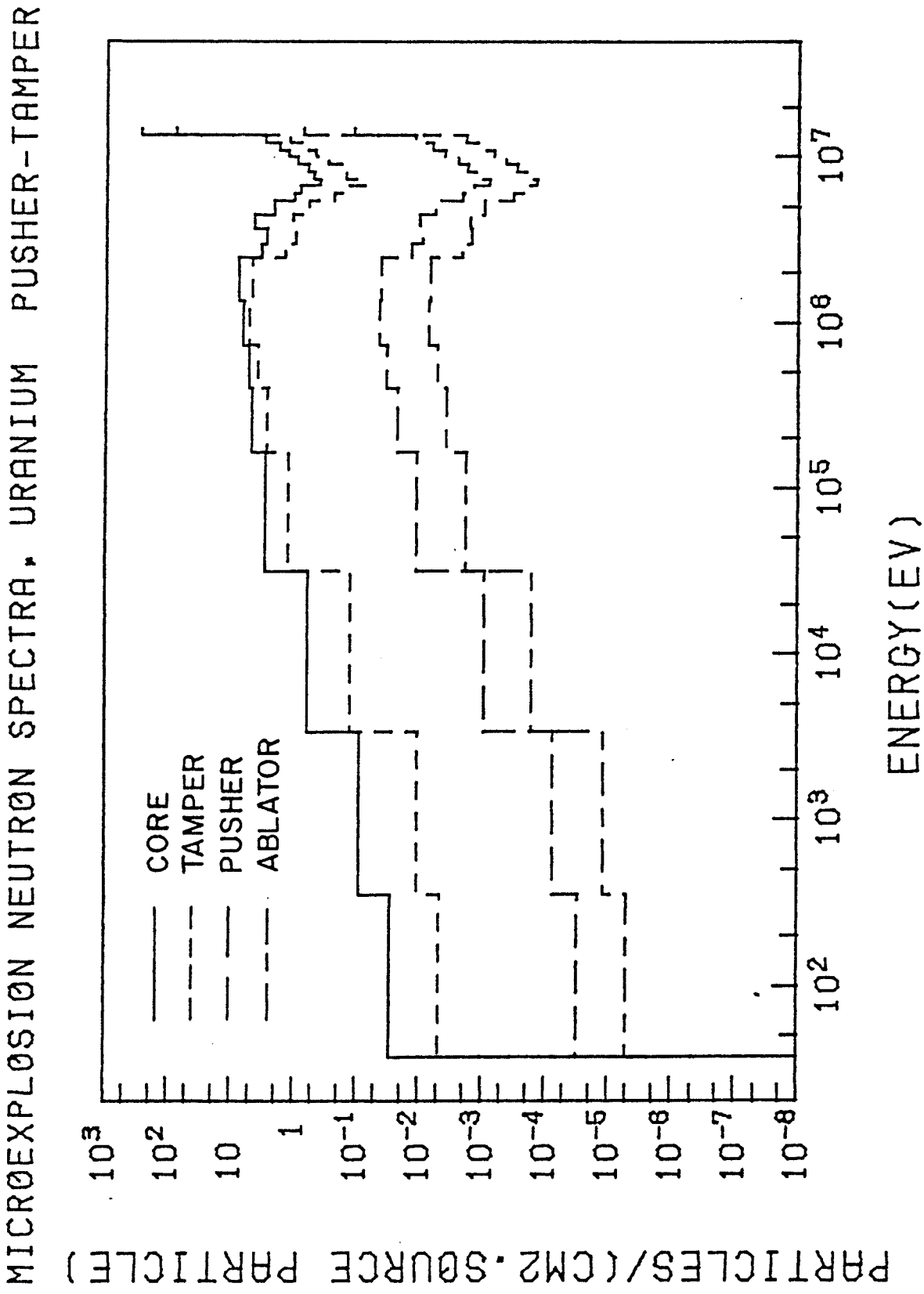
MICRØEXPLØSIØN NEUTRØN SPECTRA, URANIUM PUSHER-TAMPER
CORE
TAMPER
PUSHER
ABLATOR
PARTICLES/(CM2·SØURCE PARTICLE)
ENERGY(EV)
10^3
10^2
10
1
10^-1
10^-2
10^-3
10^-4
10^-5
10^-6
10^-7
10^-8
10^2
10^3
10^4
10^5
10^6
10^7

FIGURE 4

Table 4 Comparison of Neutron Spectra From Microexplosion for Different Pusher-Tamper Materials. Particles/(cm^2 · source neutron).

Group	Upper Energy (eV)	W				Pb				Nat. U			
		Core	Tamper	Pusher	Ablator	Core	Tamper	Pusher	Ablator	Core	Tamper	Pusher	Ablator
1	1.49+07	.29+03	.78+02	.76+00	.12+00	.29+03	.79+02	.79+00	.12+00	.29+03	.78+02	.77+00	.12.00
2	1.35+07	.28+01	.11+01	.11-01	.17-02	.32+01	.12+01	.12-01	.19-02	.31+01	.13+01	.12-01	.20-02
3	1.22+07	.18+01	.63+00	.59-02	.93-03	.22+01	.83+00	.79-02	.13-02	.19+01	.72+00	.69-02	.11-02
4	1.11+07	.13+01	.39+00	.35-02	.56-03	.11+01	.34+00	.34-02	.55-03	.13+01	.48+00	.44-02	.72-03
5	1.00+07	.75+00	.24+00	.22-02	.35-03	.94+00	.32+00	.30-02	.47-03	.92+00	.30+00	.26-02	.45-03
6	9.05+06	.56+00	.14+00	.12-02	.20-03	.58+00	.19+00	.17-02	.27-03	.64+00	.19+00	.19-02	.31-03
7	8.19+06	.38+00	.11+00	.88-03	.14-03	.43+00	.15+00	.12-02	.21-03	.51+00	.16+00	.13-02	.19-03
8	7.41+06	.38+00	.80-01	.69-03	.11-03	.56+00	.16+00	.15-02	.23-03	.42+00	.82-01	.85-03	.15-03
9	6.70+06	.65+00	.89-01	.76-03	.13-03	.56+00	.14+00	.11-02	.21-03	.84+00	.16+00	.15-02	.24-03
10	6.07+06	.10+01	.14+00	.10-02	.16-03	.14+01	.16+00	.14-02	.23-03	.10+01	.24+00	.22-02	.34-03
11	5.49+06	.24+01	.36+00	.34-02	.55-03	.17+01	.31+00	.26-02	.44-03	.22+01	.61+00	.62-02	.98-03
12	4.49+06	.33+01	.49+00	.44-02	.75-03	.34+01	.46+00	.44-02	.76-03	.46+01	.11+01	.10-01	.17-02
13	3.68+06	.20+01	.67+00	.66-02	.11-02	.15+01	.44+00	.37-02	.64-03	.30+01	.10+01	.97-02	.16-02
14	3.01+06	.20+01	.98+00	.88-02	.14-02	.12+01	.50+00	.45-02	.85-03	.35+01	.15+01	.14-01	.23-02
15	2.47+06	.49+01	.37+01	.33-01	.53-02	.52+01	.19+00	.17-01	.29-02	.82+01	.49+01	.44-01	.70-02
16	1.35+06	.39+01	.41+01	.36-01	.57-02	.23+01	.17+00	.16-01	.29-02	.68+01	.53+01	.47-01	.75-02
17	7.43+05	.30+01	.26+01	.23-01	.36-02	.17+01	.13+01	.11-01	.19-02	.54+01	.39+01	.34-01	.55-02
18	4.08+05	.24+01	.20+01	.17-01	.27-02	.13+01	.62+00	.60-02	.10-02	.48+02	.27+01	.24-01	.38-02
19	1.65+05	.88+00	.51+00	.46-02	.72-03	.44+00	.24+00	.24-02	.41-03	.30+01	.13+01	.11-01	.18-02
20	3.18+04	.10+00	.50-01	.29-03	.45-04	-	.34-01	.49-03	.76-04	.60+00	.13+00	.98-03	.16-03
21	3.35+03	-	-	-	-	-	-	-	-	.87-01	.10-01	.78-04	.12-04
22	3.54+02	-	-	-	-	-	-	-	-	.29-01	.48-02	.32-04	.50-05
23	3.73+01	-	-	-	-	-	-	-	-	-	-	-	-
24	3.93+00	-	-	-	-	-	-	-	-	-	-	-	-
25	4.14-01	-	-	-	-	-	-	-	-	-	-	-	-

Lower edge of last neutron group: 1.00-04

The neutron spectra for the three cases have the same general shape with a valley around 5 MeV. Local peaking in the pellet core at 4 and 2 MeV is caused by elastic scattering with D and T. The large peak at 14 MeV is due to neutrons escaping the pellet regions without interaction. The lower energy range contains neutrons that scattered elastically or inelastically and those produced by neutron multiplication reactions: (n,2n), (n,3n) or by fission. The W spectrum is slightly larger in magnitude than the Pb spectrum, and the natural U spectrum is larger than for either W or Pb. The natural U spectrum also extends to a lower energy range than the other two.

The gamma spectra are displayed in Figs. 5-7 and tabulated in Table 5. All spectra peak around0.5 MeV and have the same form, except for some high-energy gammas.

Table 6 compares the scalar neutron and gamma fluxes for the different cases. In the ablator region, the 14.1 MeV group flux is 83%, 82% and 78% of the total flux for the W, Pb, and natural U cases, respectively. Natural U leads to the largest scalar flux in the ablator region. The generated gamma fluxes will be largest in the W case, followed by natural U, then the Pb case.

The absorption, (n,γ) and total reaction rates are compared in Table 7. In all cases, most of the reactions occur in the tamper region. The capture in the tamper for the Pb case is less than in the W and natural U cases which leads to a larger escape of high energy neutrons to the first wall and less production of gamma rays in the pellet. The largest absorption occurs in the natural U case. For larger values of ρr for the pellet, larger interactions may be expected to occur in the pellet core.

Table 8 shows reactions of interest for the natural U pellet. Again, most of the reactions occur in the tamper region. The number of fission reactions per source neutron is 2.75×10^{-2}. The (n,γ) breeding reaction from Table 7 is 6.47×10^{-4}. This implies that if natural U is to be used in

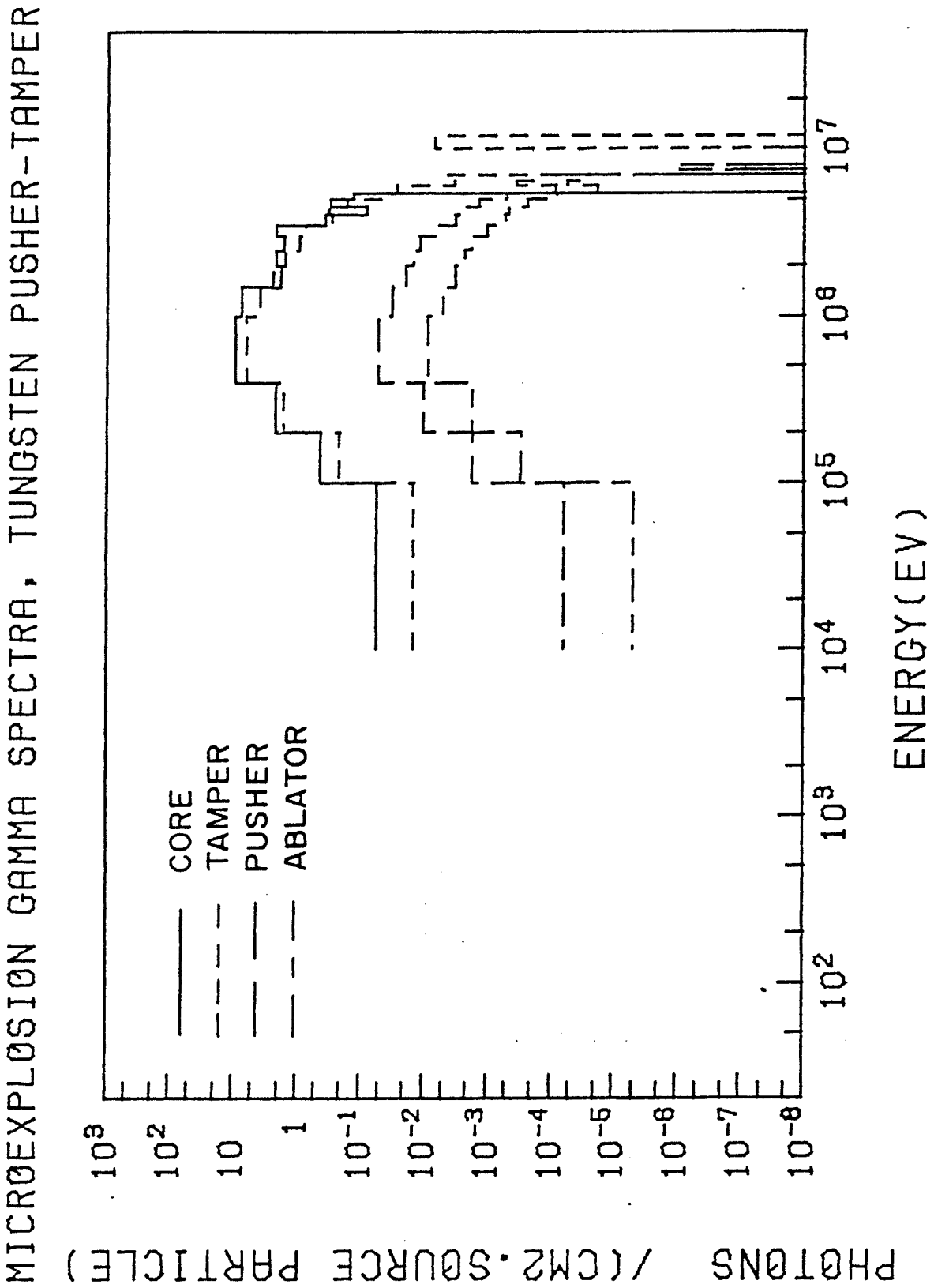
MICROEXPLOSION GAMMA SPECTRA, TUNGSTEN PUSHER-TAMPER
CORE
TAMPER
PUSHER
ABLATOR
PHOTONS /(CM2·SOURCE PARTICLE)
ENERGY(EV)
10^3
10^2
10
1
10^-1
10^-2
10^-3
10^-4
10^-5
10^-6
10^-7
10^-8
10^2
10^3
10^4
10^5
10^6
10^7
10^8

FIGURE 5

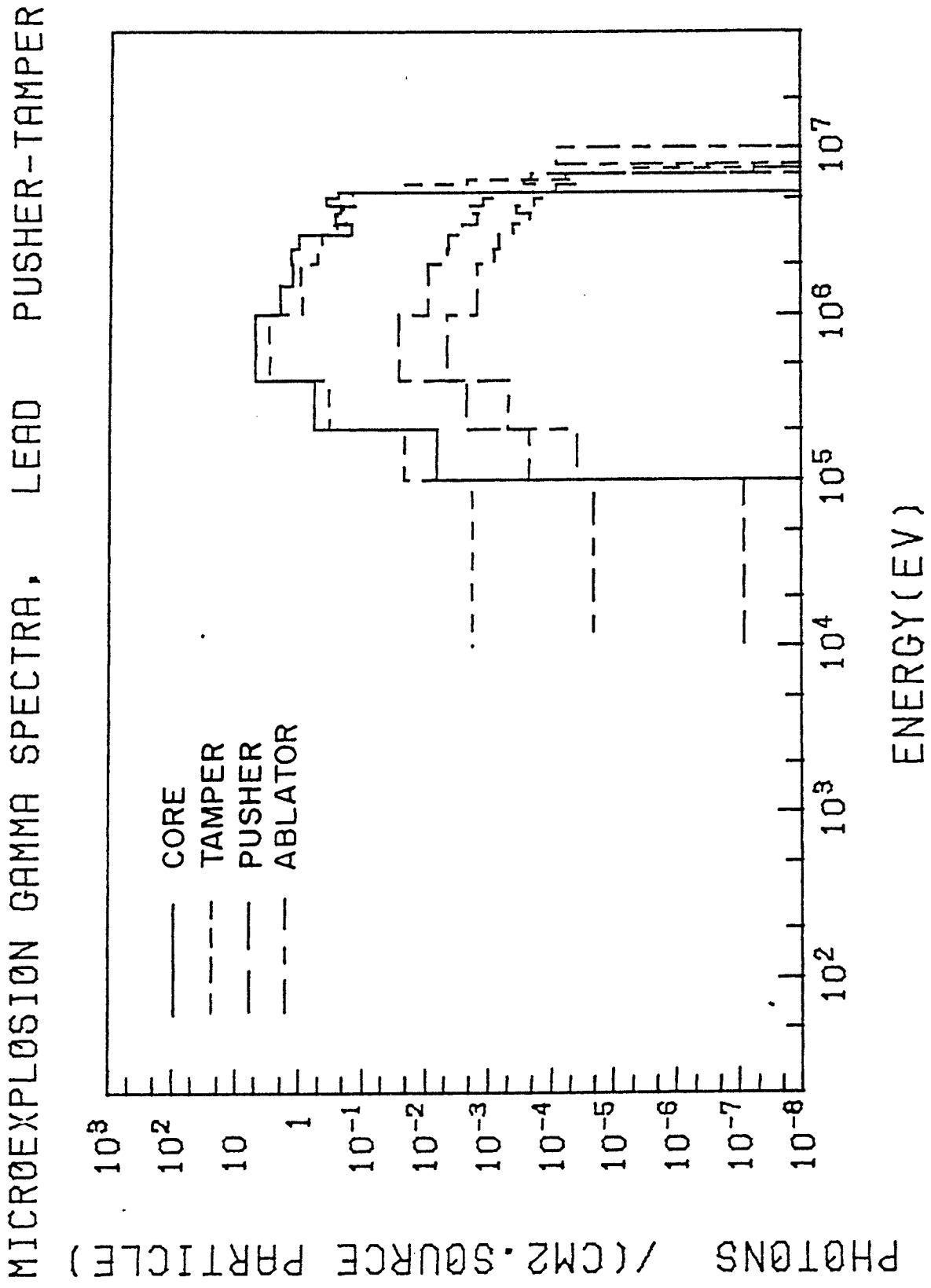
MICROEXPLOSION GAMMA SPECTRA, LEAD PUSHER-TAMPER
CORE
TAMPER
PUSHER
ABLATOR
PHOTONS /(CM2·SOURCE PARTICLE)
ENERGY(EV)
10^3
10^2
10
1
10^-1
10^-2
10^-3
10^-4
10^-5
10^-6
10^-7
10^-8
10^2
10^3
10^4
10^5
10^6
10^7

FIGURE 6

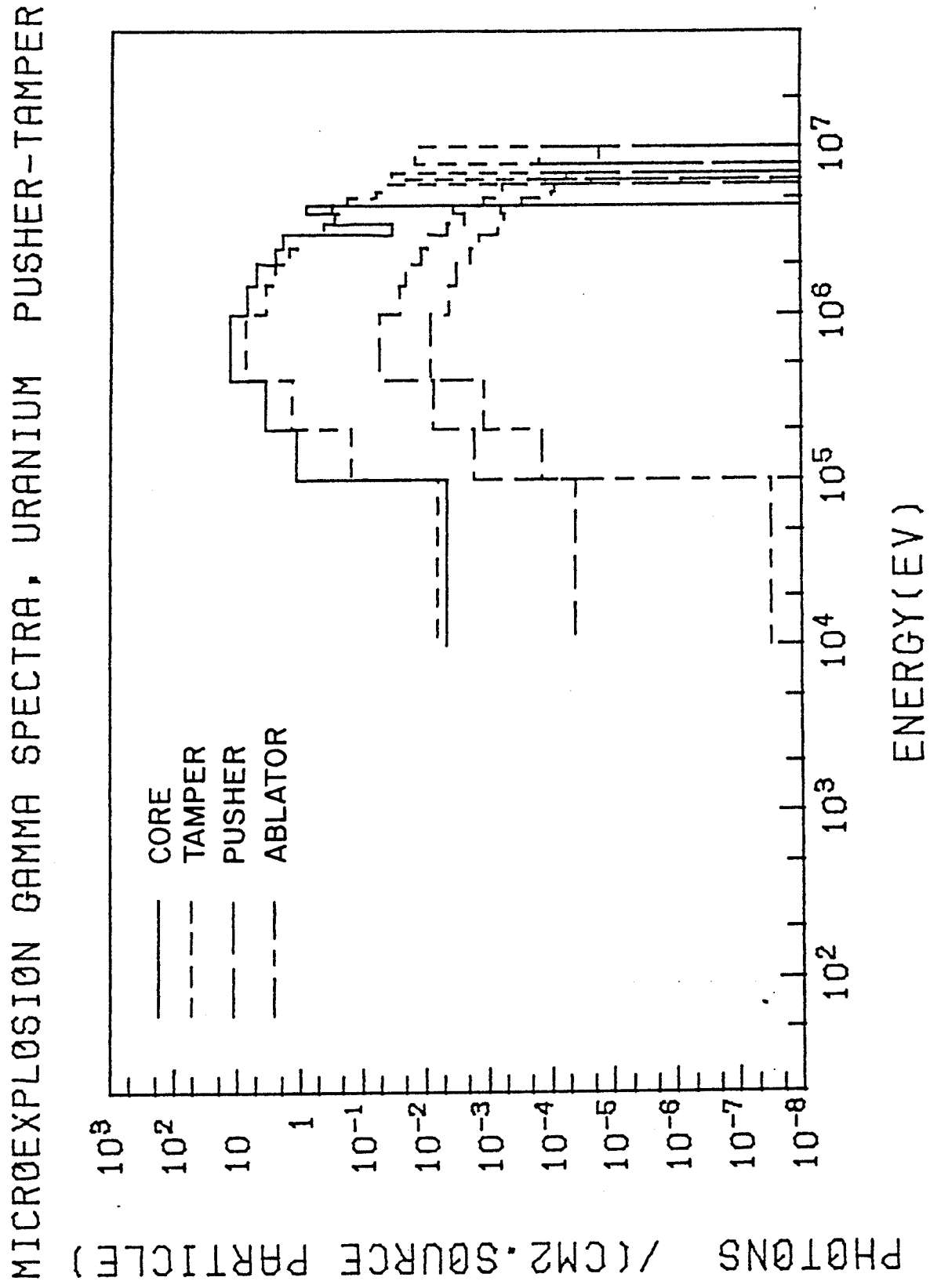
MICROEXPLOSION GAMMA SPECTRA, URANIUM PUSHER-TAMPER
CORE
TAMPER
PUSHER
ABLATOR
PHOTONS /(CM2.SOURCE PARTICLE)
ENERGY(EV)
10^3
10^2
10
1
10^-1
10^-2
10^-3
10^-4
10^-5
10^-6
10^-7
10^-8
10^2
10^3
10^4
10^5
10^6
10^7

FIGURE 7

Table 5 Comparison of Gamma Spectra From Microexplosion for Different Pusher-Tamper Materials. Photons/(cm^2 · source neutron).

Group	Upper Energy (eV)	W				Pb				Nat. U			
		Core	Tamper	Pusher	Ablator	Core	Tamper	Pusher	Ablator	Core	Tamper	Pusher	Ablator
1	1.4+07	-	-	-	-	-	-	-	-	-	-	-	-
2	1.2+07	-	.69-02	-	-	-	-	-	-	-	-	-	-
3	1.0+07	-	-	-	-	-	-	-	.86-04	-	.16-01	.16-03	.18-04
4	8.0+06	-	-	.11-05	.84-07	-	-	-	-	-	-	-	-
5	7.5+06	-	-	-	-	-	.56-05	.58-07	.92-08	-	-	-	-
6	7.0+06	-	.44-02	.17-03	.34-04	-	.40-04	.22-03	.61-04	-	.35-01	.16-03	.58-04
7	6.5+06	-	.34-02	.36-03	.55-04	-	.23-02	.29-03	.41-04	-	-	-	.24-04
8	6.0+06	-	.28-01	.85-04	.19-04	-	.22-01	.17-03	.85-04	-	.51-01	.61-03	.94-04
9	5.5+06	.13+00	.40-01	.50-03	.83-04	.24+00	.14+00	.85-03	.15-03	-	.63-01	.71-03	.10-03
10	5.0+06	.30+00	.16+00	.13-02	.24-03	.38+00	.13+00	.12-02	.19-03	-	.18+00	.12-02	.30-03
11	4.5+06	.86-01	.32+00	.28-02	.48-03	.23+00	.21+00	.22-02	.38-03	.84+00	.32+00	.37-02	.65-03
12	4.0+06	.37+00	.29+00	.31-02	.52-03	.27+00	.18+00	.15-02	.23-03	.30+00	.25+00	.26-02	.59-03
13	3.5+06	.21+01	.76+00	.63-02	.10-02	.16+00	.26+00	.27-02	.42-03	.36-01	.43+00	.46-02	.75-03
14	3.0+06	.16+01	.94+00	.11-01	.18-02	.11+01	.46+00	.46-02	.70-03	.19+01	.11+01	.94-02	.14-02
15	2.5+06	.22+01	.16+01	.14-01	.22-02	.14+01	.54+00	.47-02	.84-03	.26+01	.16+01	.12-01	.20-02
16	2.0+06	.19+01	.24+01	.20-01	.32-02	.13+01	.10+01	.92-02	.15-02	.52+01	.26+01	.21-01	.34-02
17	1.5+06	.76+01	.38+01	.32-01	.50-02	.21+01	.94+00	.91-02	.15-02	.70+01	.36+01	.27-01	.44-02
18	1.0+06	.95+01	.65+01	.54-01	.88-02	.51+01	.31+01	.28-01	.48-02	.13+02	.74+01	.55-01	.89-02
19	4.0+05	.22+01	.17+01	.11-01	.17-02	.60+00	.34+00	.23-02	.49-03	.37+01	.14+01	.78-02	.12-02
20	2.0+05	.44+00	.22+00	.17-02	.31-03	.67-02	.22-01	.23-03	.40-04	.12+01	.15+00	.17-02	.14-03
21	1.0+05	.56-01	.15-01	.61-04	.51-05	-	.19-02	.84-07	.21-04	.47-02	.68-02	.42-04	.31-07

Lower edge of last gamma group: 1.00+04

Table 6 Comparison of Neutron and Gamma Scalar Fluxes for Different Pusher-Tamper Materials. Same Final and Initial Configurations. Particles/(cm^2·source particle).

Neutron Fluxes / Region	W	Pb	Nat. U
Pellet Core	3.14+02+ (3.5) 2.84+02* (3.2)	3.10+02 (2.7) 2.85+02 (2.6)	3.42+02 (2.8) 2.90+02 (3.2)
Tamper	9.75+02 (1.9) 7.87+01 (1.9)	8.67+01 (2.8) 7.54+01 (2.7)	1.04+02 (2.0) 7.83+01 (1.9)
Pusher	1.00+00 (5.6) 8.26-01 (6.4)	9.33-01 (7.9) 8.43-01 (8.0)	9.24-01 (6.4) 6.90-01 (6.7)
Ablator	1.17-01 (9.7) 9.75-02 (10.5)	1.59-01 (7.7) 1.31-01 (8.2)	1.81-01 (7.4) 1.42-01 (7.7)
Gamma Fluxes / Region	W	Pb	Nat. U
Tamper	1.83+01 (3.4)	7.63+00 (4.9)	1.95+01 (3.7)
Pusher	1.62-01 (12.0)	8.21-02 (13.1)	1.41-01 (7.0)
Ablator	2.02-02 (19.5)	1.35-02 (20.7)	1.75-02 (16.9)

Numbers in parentheses are fractional standard deviations.
+ Total scalar flux.
* 14.1 MeV group flux.

Table 7 Absorption, (n,γ), and Total Reactions in Different Pellets. Reactions/Source Particle.

Region	Element	W Pusher-Tamper			Pb Pusher-Tamper			Nat. U Pusher-Tamper		
		Absorption	(n,γ)	Total Reactions	Absorption	(n,γ)	Total Reactions	Absorption	(n,γ)	Total Reactions
Core	^{3}T	-	-	2.84-02	-	-	2.77-02	-	-	3.11-02
	^{4}He	-	-	1.44-02	-	-	1.38-02	-	-	1.64-02
	^{2}D	2.40-07	2.40-07	2.51-02	2.38-07	2.38-07	2.38-02	2.47-07	2.47-07	2.92-02
	Subtotal	2.40-07	2.40-07	6.79-02	2.38-07	2.38-07	6.53-02	2.47-07	2.47-07	7.67-02
Tamper	Pb	-	-	-	6.10-06	6.10-06	8.52-02	-	-	-
	^{182}W	1.48-04	1.14-04	4.66-02	-	-	-	-	-	-
	^{183}W	7.51-05	5.44-05	2.60-02	-	-	-	-	-	-
	^{184}W	1.47-04	1.14-04	5.55-02	-	-	-	-	-	-
	^{186}W	1.18-04	9.62-05	5.14-02	-	-	-	-	-	-
	^{235}U	-	-	-	-	-	-	3.77-04	6.32-06	1.23-03
	^{238}U	-	-	-	-	-	-	2.53-02	5.90-04	1.66-01
	Subtotal	4.88-04	3.79-04	1.80-01	6.10-06	6.10-06	8.52-02	2.57-02	5.96-04	1.67-01
Pusher	Pb	-	-	-	5.72-07	5.72-07	8.27-03	-	-	-
	^{182}W	1.32-05	1.00-05	4.37-03	-	-	-	-	-	-
	^{183}W	6.72-06	4.73-06	2.44-03	-	-	-	-	-	-
	^{184}W	1.32-05	1.00-05	5.21-03	-	-	-	-	-	-
	^{186}W	1.06-05	8.52-06	4.82-03	-	-	-	-	-	-
	^{235}U	-	-	-	-	-	-	3.58-05	5.44-07	1.12-04
	^{238}U	-	-	-	-	-	-	2.42-03	5.06-05	1.55-02
	Subtotal	4.37-05	3.33-05	1.68-02	5.72-07	5.72-07	8.27-03	2.47-03	5.11-05	1.56-02
Ablator	Fe	4.18-04	1.75-06	7.30-03	4.35-04	1.15-06	6.99-03	4.25-04	2.47-06	8.11-03
TOTAL		9.50-04	4.13-04	2.72-01	4.42-04	6.91-06	1.66-01	2.86-02	6.47-04	2.67-01

Table 8 Fission Reactions in the Nat. U Pellet. Reactions/Source Particle.

Region	Element	$\langle\psi,\nu\rangle^{+}$	$\langle\psi,\Sigma_f\rangle$	$\langle\nu\Sigma_f,\psi\rangle$
Tamper	^{235}U	7.59-04	3.71-04	1.54-03
	^{238}U	1.06-01	2.47-02	1.08-01
	Subtotal	1.07-01	2.51-02	1.10-01
Pusher	^{235}U	7.21-05	3.52-05	1.47-04
	^{238}U	1.00-02	2.37-03	1.04-02
	Subtotal	1.01-02	2.41-03	1.05-02
TOTAL		1.17-01	2.75-02	1.21-01

+$\langle$, $\rangle$ denotes an inner product over space, time, and energy for the flux ψ and the response function of interest. ν is the average number of neutrons emitted per fission event, and Σ_f is the macroscopic fission cross section.

a pellet, breeding in the pellet is not possible. What is possible is neutron multiplication (1.17×10^{-1} fission particle/source particle from Table 8), and energy multiplication: 200 MeV/fission reaction, which corresponds to $200 \times 2.75 \times 10^{-2} = 5.50$ MeV/source particle. This is quite substantial, given that the blanket heating amounts to about 16 MeV/source particle.

The (n,2n) and (n,3n) reactions for different pellets are shown in Table 9. The largest number of (n,2n) reactions occurs with W; even more than for Pb. The (n,3n) reaction from natural U is quite substantial compared to the cases of W and Pb. A neutron balance is shown in Table 10, using the relationship:

$$\text{Neutron Leakage} = \text{Source} + 1 \cdot R(\sigma_{n,2n}) + 2 \cdot R(\sigma_{n,3n}) + R(\nu\sigma_f) - R(\sigma_a) \qquad (1)$$

where:

$\sigma_a = \sigma_c + \sigma_f$,

$\sigma_c = \sigma_{n,\gamma} + \sigma_{n,\alpha} + \sigma_{n,p} + \sigma_{n,d} + \cdots$,

$R(\sigma)$ denotes a given reaction rate,

σ denotes a given reaction.

Notice that a convention used in multigroup cross section sets is adopted: the absorption cross section (σ_a) is defined as the sum of the fission (σ_f) and capture (σ_c) cross sections. The latter include all neutron disappearance reactions except for the (n,2n), (n,3n) and (n,f) reactions. It is clear that natural U leads to 14% neutron multiplication, mostly from fissions, whereas W leads to 7% multiplication, and Pb to 4%. This is inferred from the particle leakage from the pellet.

Table 11 gives approximate estimates of the neutron and gamma energy leakages per source neutron from different pellets, calculated according to the relationship:

$$E = S \sum_{g=1}^{G} \phi^g E^g_{mid}, \qquad (2)$$

Table 9 The (n,2n) and (n,3n) Reactions for Different Pellets. Reactions/Source Neutron.

Region	Element	W Pusher-Tamper		Pb Pusher-Tamper		Nat. U Pusher-Tamper	
		(n,2n)	(n,3n)	(n,2n)	(n,3n)	(n,2n)	(n,3n)
Core	^{3}T	1.23-03	-	1.23-03	-	1.23-03	-
	^{4}He	-	-	-	-	-	-
	^{2}D	4.50-03	-	4.50-03	-	4.50-03	-
	Subtotal	5.73-03	-	5.73-03	-	5.73-03	-
Tamper	Pb	-	-	3.01-02	4.46-04	-	-
	^{182}W	1.58-02	1.22-07	-	-	-	-
	^{183}W	8.76-03	2.58-06	-	-	-	-
	^{184}W	1.87-02	6.51-04	-	-	-	-
	^{186}W	1.76-02	2.72-04	-	-	-	-
	^{235}U	-	-	-	-	4.32-05	5.05-06
	^{238}U	-	-	-	-	1.70-02	1.02-02
	Subtotal	6.09-02	9.26-04	3.01-02	4.46-04	1.70-02	1.02-02
Pusher	Pb	-	-	2.94-03	4.38-05	-	-
	^{182}W	1.51-03	1.17-08	-	-	-	-
	^{183}W	8.39-04	2.47-07	-	-	-	-
	^{184}W	1.79-03	4.30-06	-	-	-	-
	^{186}W	1.68-03	2.61-05	-	-	-	-
	^{235}U	-	-	-	-	4.15-06	4.87-07
	^{238}U	-	-	-	-	1.63-03	9.83-04
	Subtotal	5.82-03	3.07-05	2.94-03	4.38-05	1.63-03	9.83-04
Ablator	Fe	9.99-04	-	1.04-03	-	1.01-03	-
TOTAL		7.34-02	9.57-04	3.98-02	4.90-04	2.44-02	1.12-02

Table 10 Neutron Balances for Different Pellets

	Leakage	Source	$1 \cdot R(\sigma_{n,2n})$	$2 \cdot R(\sigma_{n,3n})$	$R(\nu\sigma_f)$	$R(\sigma_a)$
W Pellet	1.07+00	1	7.34-02	1.91-03	-	9.50-04
Pb Pellet	1.04+00	1	3.98-02	9.80-04	-	4.42-04
Nat. U Pellet	1.14+00	1	2.44-02	2.24-02	1.21-01	2.86-02

Table 11 Comparison of Neutron and Gamma Energy Leakages from Different Pellets (MeV/Source Particle)

	W Pellet	Pb Pellet	Natural U Pellet
Neutron Energy Leakage	12.68	12.67	12.84
Gamma Energy Leakage	0.27	0.14	0.26
Fission Energy Generation	----	-----	5.50

where:

E^g_{mid} is the midpoint energy of each group g for either neutrons or gammas (MeV),

ϕ^g is the group flux in particles/(cm^2·source particle),

S is a spherical surface taken at the midpoint of the ablator region.

The results of Tables 10 and 11 show that the 14.1 MeV energy of the neutrons born in the pellet suffers a loss, but the number of neutrons leaving the pellet is multiplied. In the case of the Uranium pellet, an extra 5.5 MeV of energy per source neutron is obtained by fast fission. The energy loss in the pellet will affect pellet phenomena and must be accounted for in detailed pellet calculations. Eventually, it will reappear in some other form in the cavity. The 5.5 MeV fission energy will be mostly kinetic energy of fission products which can deposit their energy in the pellet plasma or the cavity-filled gas. Thus, provisions must be taken to extract the energy deposited in the cavity buffer gas.

The next section considers the coupled pellet-blanket calculations and results.

III. Coupled Pellet-Blanket Neutronics and Photonics

III.1. Introduction

The particle interactions in the pellet material and the ensuing neutron and gamma spectra will affect the breeding, heating, and radiation damage estimates in the blanket. Previous models of inertial confinement systems considered a pure 14.1 MeV neutron source as arising from pellet micro-explosions[3,6,15-17] even though recognizing the necessity to take the pellet interaction effects into consideration in future studies. In the following, coupled pellet-blanket calculations are compared to a calculation considering a pure 14.1 MeV neutron source. The latter would also represent a magnetic confinement neutron source.

III.2. Pellet-Blanket Computational Model

A Li_2O blanket is considered to surround the reactor cavity with a radius of 5m. The blanket composition and configuration are shown in Fig. 8. Calculations for this blanket have been previously extensively documented.[6,13] In these earlier calculations, however, a pure 14.1 MeV neutron source was used without accounting for the effects of the pellet composition. Li_2O has a high Li atomic density compared to other Li solid compounds and does not need enrichment in ^6Li to attain sufficient breeding. Its use as micro-particles would help attenuate the blast wave generated by the micrexplosion in the high density fill gas used in the reactor cavity. A stainless steel structure and a boron carbide and stainless steel shield are used. The nuclide densities are shown in Table 12.

Spectra from pellets with W, Pb and natural U as pusher-tamper materials were incident on the first wall. The corresponding breeding, heating and radiation damage data will be compared to those obtained by a pure 14.1 MeV neutron as a source model and to each other.

III.3. Calculational Results

Table 13 shows the scalar fluxes for the cases of W, Pb and natural U as tamper-pusher materials and compares them to the case of a pure 14.1 MeV source neutron flux. The 14.1 MeV group flux is shown separately. At the first wall, the scalar flux for the cases of W and natural U are slightly higher than if a pure 14.1 MeV source were used because of the neutron multiplication. However, the fraction of 14.1 MeV group flux in the total flux is ~ 16% when a pure 14.1 MeV flux is used, whereas it is ~ 11% with natural U as tamper-pusher, ~ 13% in the case of Pb, and ~ 12% in the case of W. Thus, there is a clear softening of the spectrum. Let us remember that our pellet core has a low ρr value of 0.94. For higher core ρr pellets this effect will be much more pronounced and must be accounted

MATERIALS IDENTIFICATION

1 GRAPHITE
2 STAINLESS STEEL (100% d.f)
3 Li_2O (60%) + S.S. (2%)
4 B_4C (90%) + S.S. (10%)
1000 INNER VACUUM
0 OUTER VACUUM

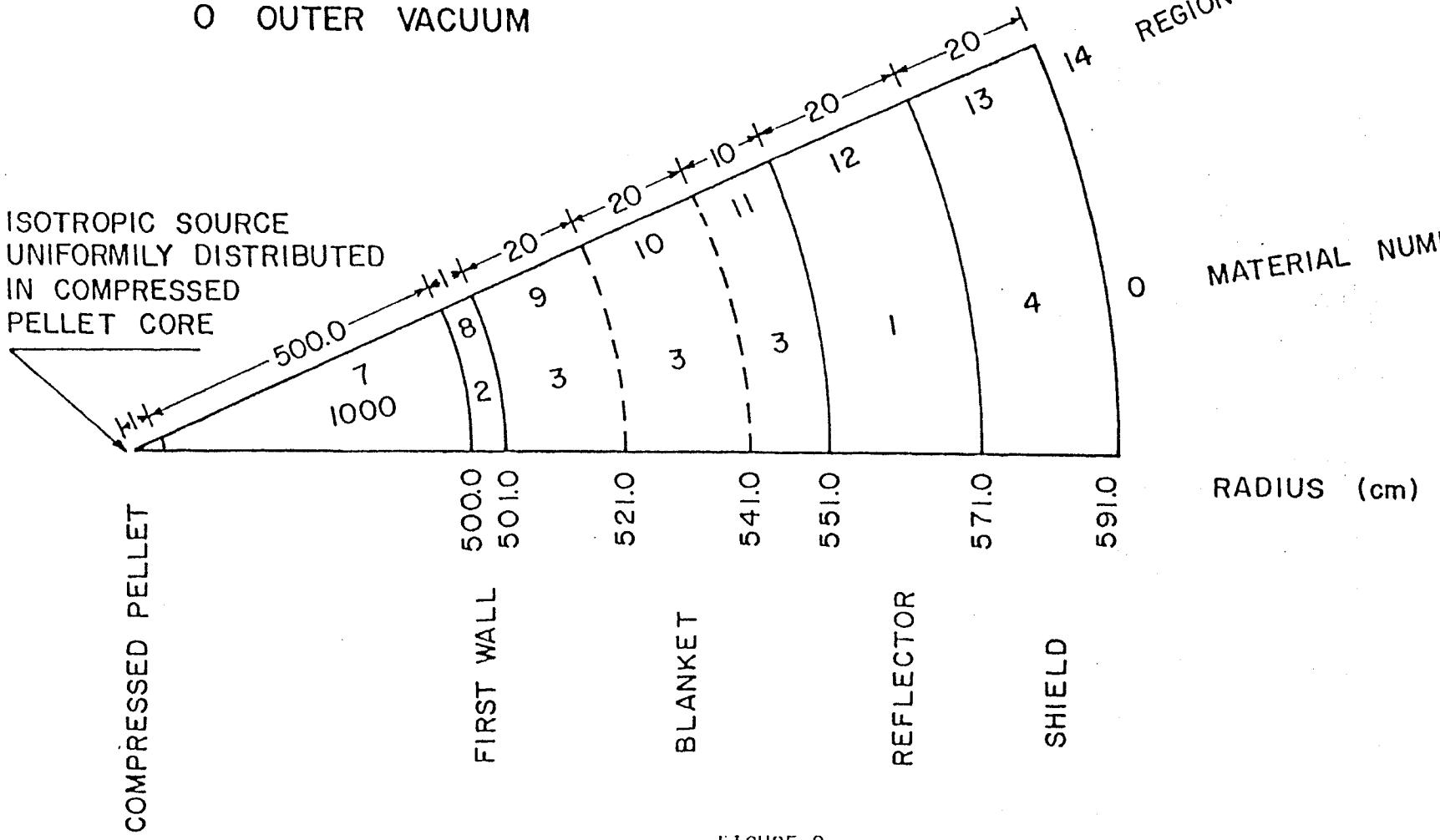

FIGURE 8

Table 12 Material Compositions Used in the Blanket and Shield Model

	Medium	Constituent Elements	Nuclei Densities Nuclei/(barn·cm)
5	Stainless Steel (S.S.) First Wall	Cr	0.145-01
		Ni	0.938-02
		Fe	0.614-01
6	Blanket 60 v/o Li_2O + 2 v/o S.S.	^{6}Li	0.365-02
		^{7}Li	0.455-01
		^{16}O	0.246-01
		Cr	0.290-03
		Ni	0.188-03
		Fe	0.123-02
7	Graphite Reflector	^{12}C	0.804-01
8	Shield 90 v/o B_4C + 10 v/o S.S.	^{12}C	0.247-01
		^{10}B	0.196-01
		^{11}B	0.793-01
		Cr	0.145-02
		Ni	0.938-03
		Fe	0.614-02

Table 13 Comparison of Neutron Scalar Fluxes in Blanket Regions for Different Pellet Compositions. Neutrons/(cm^2·source particle).

Region	Pusher-Tamper Material			Pure 14.1 MeV Source
	W	Pb	Nat. U	
First Wall	2.20-06[+] (1.3) 2.72-07* (2.7)	2.09-06 (3.5) 2.73-07 (4.7)	2.39-06 (2.3) 2.68-07 (4.0)	2.10-06 (3.3) 3.29-07 (4.5)
Blanket				
Zone 1	1.63-06 (0.7) 1.24-07 (0.9)	1.59-06 (1.6) 1.30-07 (1.6)	1.77-06 (1.7) 1.17-07 (1.9)	1.54-06 (1.2) 1.42-07 (1.5)
Zone 2	7.73-07 (8.9) 2.47-08 (2.8)	7.73-07 (2.5) 2.60-08 (4.7)	8.54-07 (1.4) 2.68-08 (5.9)	7.60-07 (1.9) 2.62-08 (6.6)
Zone 3	4.06-07 (1.8) 6.00-09 (8.0)	4.28-07 (3.8) 6.19-09 (14.4)	4.60-07 (3.9) 7.73-09 (14.8)	4.21-07 (4.1) 7.13-09 (12.6)
Reflector	2.24-07 (2.3) 1.84-09 (10.8)	2.48-07 (3.1) 3.06-09 (14.3)	2.45-07 (5.5) 1.87-09 (15.2)	2.21-07 (6.0) 1.84-09 (15.3)
Shield	1.55-08 (4.3) 2.70-10 (19.5)	1.62-08 (12.8) 6.62-10 (38.2)	1.33-08 (10.7) 2.32-10 (41.7)	1.64-08 (10.0) 3.66-10 (40.7)

+ Total scalar flux.

* 14.1 MeV group flux.

Numbers in parentheses are percentage fractional standard deviations.

for in the blanket design. In Table 14, for the gamma fluxes, an interesting result appears. The gamma fluxes at the first wall from the pellet calculations compare in magnitude to the one for the pure 14.1 MeV source, except for the Pb case. This implies that the gammas produced in the pellet tamper-pusher just balance those that would have been produced at the first wall if the neutrons had not interacted with the pellet materials.

The effect of pellet interactions of the neutrons on tritium breeding is shown in Table 15. The contribution to tritium production from ^{7}Li, a fast neutron reaction, is less in all pellet cases compared to the pure 14.1 MeV case. On the opposite end, the contribution from reactions with ^{6}Li, a slow neutron reaction, is substantially larger compared to the pure 14.1 MeV case. On balance, all cases give nearly equal total tritium breeding ratios except for the effect of neutron multiplication which increases the production in the case of a natural U pusher-tamper by about 8% compared to the W case.

The effect on the radiation damage at the stainless steel first wall (5m radius) and in the graphite at the reflector in terms of average displacements per atom per sec is displayed in Table 16. The spectrum softening in the case of Pb leads to less damage, but in the case of natural U, it is counterbalanced by the larger multiplication. Thus dpa values per source particle compare in magnitude to the case of the pure 14.1 MeV source. The effect on the helium production rate (per source particle) at the first wall is more pronounced as shown in Table 17: the spectrum softening in the pellet leads to less helium production for all the pellet cases than in the pure 14.1 MeV source case. It is less by ~17 % in the natural U pusher-tamper case compared to the pure 14.1 MeV cases and less by ~7% compared to the W case. The hydrogen production (per source particle) is also less in the pellet cases than the pure 14.1 MeV source case. If these reductions in radiation damage values can be made larger, for example, by larger softening of the

Table 14 Comparison of Gamma Scalar Fluxes in Blanket Regions for Different Pellet Compositions. Photons/(cm^2·source particle).

Region	Pusher-Tamper Material			Pure 14.1 MeV Source
	W	Pb	Nat. U	
First Wall	7.71-07 (1.9)	6.90-07 (4.9)	7.94-07 (4.6)	7.64-07 (4.1)
Blanket				
Zone 1	5.61-07 (1.2)	5.28-07 (3.0)	5.66-07 (2.7)	5.34-07 (2.6)
Zone 2	2.69-07 (1.5)	2.49-07 (3.0)	2.72-07 (2.8)	2.48-07 (2.5)
Zone 3	1.40-07 (1.8)	1.27-07 (4.7)	1.40-07 (4.6)	1.31-07 (4.0)
Reflector	8.64-08 (2.8)	8.14-08 (6.4)	8.82-08 (4.4)	7.65-08 (3.9)
Shield	3.35-08 (2.8)	3.60-08 (6.4)	3.47-08 (6.1)	3.74-08 (7.0)

Numbers in parentheses are percentage fractional standard deviations.

Table 15 Comparison of Tritium Production Per Source Neutron for Different Pellet Compositions in Blanket Region. (Tritons/source particle).

Zone	W Pusher-Tamper	Pb Pusher-Tamper	Nat. U Pusher-Tamper	Pure 14.1 MeV Source
	^{7}Li Contribution			
1	2.79-01±2.88-03	2.57-01±5.07-03	2.78-01±6.88-03	3.11-01±4.93-03
2	1.05-01±1.90-03	9.88-02±4.91-03	1.04-01±5.42-03	1.11-01±4.36-03
3	2.06-02±7.28-04	1.79-02±1.54-03	2.01-02±1.56-03	2.14-02±1.17-03
Subtotal	4.05-01±3.53-03	3.74-01±7.22-03	4.02-01±8.90-03	4.43-01±6.68-03
	^{6}Li Contribution			
1	4.16-01±3.89-03	3.88-01±7.83-03	4.64-01±8.32-03	3.71-01±5.58-03
2	2.59-01±2.57-03	2.51-01±4.66-03	2.91-01±4.92-03	2.43-01±4.80-03
3	1.13-01±1.67-03	1.18-01±3.79-03	1.28-01±3.65-03	1.09-01±3.42-03
Subtotal	7.88-01±4.95-03	7.57-01±9.91-03	8.73-01±1.03-02	7.23-01±8.12-03
Total	1.19+00±6.08-03	1.13+00±1.23-02	1.28+00±1.36-02	1.17+00±1.05-02

Table 16 Comparison of Atomic Displacement Values for Different Pellet Compositions (dpa/sec).

Region	W	Pb	Nat. U	Pure 14.1 MeV Source
First Wall	5.13-08±8.65-10	5.00-08±4.51-09	5.22-08±1.41-09	5.40-08±2.35-09
Graphite Reflector	2.82-09±9.93-11	3.09-09±1.81-10	3.03-09±2.16-10	2.99-09±2.00-10

For a microexplosion yield of 100 MJ at a repetition rate of 1 Hz, the 14.1 MeV neutron source strength is 3.55×10^{19} (neutrons/sec). First wall radius is 5 m.

Table 17 Comparison of Gas Production Values in First Wall and Reflector for Different Pellet Compositions. (appm/sec).

Region	W	Pb	Nat. U	Pure 14.1 MeV Source
	Hydrogen Production			
First Wall	2.45-06±5.64-08	2.42-06±8.71-08	2.39-06±7.01-08	2.77-06±1.16-07
	Helium Production			
First Wall	8.67-07±2.17-08	8.60-07±3.48-08	8.40-07±2.58-08	1.01-06±4.54-08
Reflector	1.53-07±9.04-09	2.08-07±1.78-08	1.51-07±1.84-08	1.63-07±1.50-08

For a microexplosion yield of 100 MJ at a repetition rate of 1 Hz, the 14.1 MeV source strength is 3.55×10^{19} (neutrons/sec). First wall radius is 5 m.

spectrum using larger ρr values, then this may become an interesting neutron damage first-wall protection scheme. This is possible, provided protection of the wall from pellet debris is feasible, for example, by use of a dense cavity fill-gas.

We now consider the nuclear energy deposition in the blanket. As shown in Table 18, the heat deposition in the first wall is decreased for all cases of coupled pellet calculations because of the spectral softening. However, the overall neutron heating in the blanket is largest in the natural U case because of the neutron multiplication. The gamma heating at the first wall is highest in the natural U case and lowest for the Pb case. The same trend occurs for the total gamma heating. Overall, Pb leads to the least heating at the first wall, and natural U the largest. The total heating in MeV per source neutron in the cases of Pb and W is 15.7; not much different from the one which would be estimated using a pure 14.1 MeV neutron source. The case of natural U leads to a higher heating rate in the blanket: 16.4 MeV/source neutron. Added to this is the energy released by fissioning in the pellet already estimated as 5.5 MeV/source neutron. This is a total of 21.9 MeV/fusion, and is a ~ 39% increase in energy production compared to the W and Pb cases. Thus, natural U would offer the chance of using to our advantage the interactions in the pellet for energy multiplication and neutron multiplication. The latter would lead to higher breeding in the blanket. It may be possible to use depleted uranium or thorium instead of natural U for moderate neutron and energy multiplication in the pellet.

The radiation damage parameters per unit of yearly thermal energy produced are shown in Table 19. Compared to a 14.1 MeV neutron source, the W and Pb pellets show a slight reduction in energy production, but the U pellet leads to a substantial increase in energy production. If the average atomic displacements are the determining factor for first wall replacement, then

Table 19 Radiation Damage Parameters at the First Wall per Unit Thermal Energy Produced for Different Pellets

	W	Pb	Natural U	Pure 14.1 MeV Source
Thermal Power [MWth]	89.3	89.3	124.5	90.42
Atomic Displacements [dpa/(MWth.year)]	1.81-02	1.76-02	1.32-02	1.88-02
Hydrogen Production [appm/(MWth.year)]	8.64-01	8.54-01	6.05-01	9.65-01
Helium Production [appm/MWth.year)]	3.06-01	3.03-01	2.13-01	3.52-01

First Wall radius is 5 m.

Table 18 Comparison of Nuclear Energy Deposition for Different Pellet Compositions. (MeV/source neutron).

Region	W	Pb	Nat. U	Pure 14.1 MeV Source
	Neutron Heating			
First Wall	3.36-01±7.63-03	3.31-01±1.19-02	3.28-01±9.01-03	3.81-01±1.59-02
Blanket 1	6.91+00±3.94-02	6.90+00±9.30-02	7.20+00±1.10-01	7.11+00±6.95-02
2	3.08+00±2.85-02	3.15+00±8.55-02	3.28+00±5.75-02	3.10+00±7.14-02
3	9.13-01±1.64-02	9.45-01±3.42-02	1.00+00±3.74-02	9.05-01±3.33-02
Reflector	2.78-01±1.08-02	3.33-01±2.25-02	2.92-01±2.78-02	3.00-01±1.63-02
Subtotal	1.15+01±5.30-02	1.17+01±1.33-01	1.21+01±1.33-01	1.18+01±1.07-01
	Gamma Heating			
First Wall	1.23+00±2.31-02	1.12+00±6.20-02	1.30+00±6.37-02	1.21+00±4.60-02
Blanket 1	1.50+00±1.60-02	1.45+00±4.73-02	1.55+00±5.38-02	1.50+00±3.86-02
2	8.21-01±1.27-02	7.62-01±2.36-02	8.17-01±3.11-02	7.63-01±1.97-02
3	2.39-01±5.95-03	2.10-01±1.16-02	2.20-01±1.20-02	2.20-01±1.11-02
Reflector	4.35-01±1.12-02	4.24-01±2.65-02	4.53-01±2.31-02	4.04-01±2.02-02
Subtotal	4.23+00±3.33-02	3.97+00±8.65-02	4.34+00±9.27-02	4.10+00±6.73-02
	Total Heating			
First Wall	1.57+00±2.43-02	1.45+00±6.31-02	1.63+00±6.43-02	1.59+00±4.87-02
Blanket 1	8.41+00±4.26-02	8.35+00±1.04-01	8.75+00±1.22-01	8.61+00±8.00-02
2	3.90+00±3.12-02	3.91+00±8.87-02	4.10+00±6.54-02	3.86+00±7.41-02
3	1.15+00±1.74-02	1.16+00±3.61-02	1.22+00±3.93-02	1.13+00±3.51-02
Reflector	7.13-01±1.56-02	7.57-01±3.48-02	7.45-01±3.61-02	7.04-01±2.60-02
TOTAL	1.57+01±6.26-02	1.57+01±1.59-01	1.64+01±1.62-01	1.59+01±1.26-01

the natural U pellet leads in principle to wall lifetimes about 30% longer than in the case of a pure 14.1 MeV source for the same energy production. On the basis of helium production wall lifetimes 40% longer can be expected. This analysis depends, of course, on average time-integrated values and must be supplemented by time-dependent studies. These rate effects are being studied and will be reported in the future.

IV. Conclusions and Recommendations

Neutronics and photonics calculations for a low core ρr, low gain pellet for electron-beam fusion were undertaken. The neutron interactions in the pellet and their effect on the breeding, heating, and radiation damage estimates in the blanket justify the adoption of the calculational model over the previously used one of a pure 14.1 MeV neutron source emerging from the pellet microexplosion. Development of improved models which simultaneously couple the hydrodynamics calculations to the neutronics and photonics is recommended for better estimates. It is shown that breeding in natural U cannot be achieved in the pellet because of the predominance of fission reactions. However, substantial neutron multiplication, and energy multiplication can be achieved with the use of natural U. The problems associated with activation and fission products released in the reactor cavity need to be investigated for this case. Breeding and heating rates in the blanket are not greatly affected by neutron interactions in the pellet for the W and Pb cases, but the relative contributions from different reactions (^{6}Li,^{7}Li) and the spatial distribution of the heating are affected. Per unit of energy produced, the atomic displacements and gas production rates at the first wall are reduced compared to a pure 14.1 MeV source case. This means longer first wall lifetimes for a given amount of produced energy. This is particularly true for the natural U pellet. For larger ρr pellets (if feasible), these effects are expected to be more pronounced. Since the system is a pulsed

one in nature, there is a need to estimate in future work the time dependence of heat deposition and radiation atomic displacement and their impact on the structural design of the blankets and shields for such systems.

Acknowledgements

Discussions with Professor G.L. Kulcinski with the first author are greatly appreciated. Thanks are due to Mr. T. Wu from the University of Wisconsin for cross-section data handling. The manuscript preparation by Mrs. Sarah Cohen and Miss Gail Herrington is appreciated. This work was prepared on account of work partly sponsored by Sandia Laboratories for the U.S. Department of Energy (USDOE).

References

1. G. Yonas, "Fusion Power With Particle Beams", Scientific American, V. 231, N.5 (Nov. 1978).

2. R.W. Conn, et al., "SOLASE, a Conceptual Laser Fusion Reactor Design," University of Wisconsin, UWFDM-220 (Dec. 1977).

3. M.M.H. Ragheb, A.C. Klein and C.W. Maynard, "Shielding Study of a Laser Fusion Reactor Mirror and Beam Duct System", Trans. Am. Nucl. Soc. (June 1979).

4. J. Nuckolls, L. Wood, A. Thiessen, and G. Zimmerman, "Laser Compression of Matter to Super-High Densities: Thermonuclear (CTR) Applications", Nature, Vol. 239 (Sept. 1972).

5. S.G. Varnado and G.A. Carlson, "Considerations in the Design of Electron-Beam-Induced Fusion Reactor Systems", Nuclear Technology, Vol. 29 (June 1976).

6. M.M.H. Ragheb, E.T. Cheng, and R.W. Conn, "Monte Carlo Study of Asymmetric Effects in a Magnetically-Protected-First Wall Laser Driven Reactor", Atomkernenergie (ATKE), 31, Lfg. 4, p. 217 (1978).

7. M.M.H. Ragheb, E.T. Cheng, and R.W. Conn, "Monte Carlo and Discrete Ordinate Investigations for a Laser Reactor Li_2O Blanket", Atomkernenergie (ATKE), 31, Lfg. 3, p. 192 (1978).

8. N. Ghoniem and G.L. Kulcinski, "Swelling of Metals Under Pulsed Irradiation", Fusion Research Program, Univ. of Wisconsin, UWFDM-179 (Oct. 1976).

9. F. Beranek, "Time-Dependent Neutronics Studies in Inertial Confinement Fusion", Ph.D. Thesis, Univ. of Wisconsin-Madison (May 1978).

10. G.A. Moses and G. Magelssen, "PHD-IV, A Plasma Hydrodynamics - Thermonuclear Burn - Radiative Transfer Computer Code", Fusion Research Program, Univ. of Wisconsin-Madison, UWFDM-194 (1977).

11. RSIC Code Package CCC-203, "MORSE-CG", Radiation Shielding Information Center, ORNL (Sept. 1976).

12. M.M.H. Ragheb and C.W. Maynard, "Monte Carlo Statistical Weighting Methods for External-Source-Driven Multiplying Systems", Proc. Conf. on Computational Methods in Nuclear Engineering, American Nuclear Society (April 1979).

13. M.M.H. Ragheb, E.T. Cheng, and R.W. Conn, "Comparative One-Dimensional Monte Carlo and Discrete Ordinates Neutronics and Photonics Analysis for a Laser Fusion Reactor Blanket With Li_2O Particles as Coolant and Breeder", Fusion Research Program, Univ. of Wisconsin-Madison, UWFDM-193 (Jan. 1977).

14. RSIC Data Collection, DLC-41B, "VITAMIN-C" (1978).

15. M.M.H. Ragheb, M.Z. Youssef, S.I. Abdel-Khalik, and C.W. Maynard, "Three-Dimensional Lattice Calculations for a Laser Fusion Fissile-Enrichment Fuel Factory", Trans. Am. Nucl. Soc., 30, 59 (Nov. 1978).

16. M.M.H. Ragheb, M.Z. Youssef, S.I. Abdel-Khalik, and C.W. Maynard, "Three-Dimensional Neutronics Analysis of the SOLASE-H Laser Fusion Fissile-Enrichment-Fuel-Factory", UWFDM-266, Univ. of Wisconsin (1978).

17. L.A. Booth, "Central Station Power Generation by Laser-Driven Fusion", LA-4858-MS, Vol. 1 (Feb. 1972).

List of Tables

List of Figures